REVIEW SUMMARY

NANOPARTICLES

Nonadditivity of nanoparticle interactions

Carlos A. Silvera Batista, Ronald G. Larson,* Nicholas A. Kotov*

BACKGROUND: Interactions between inorganic nanoparticles (NPs) are central to a wide spectrum of physical, chemical, and biological phenomena. An understanding of these interactions is essential for technological implementation of nanoscale synthesis and engineering of self-organized NP superstructures with various dimensionalities, collective properties at the nanoscale, and predictive biological responses to NPs. However, the quantitative description of NP forces encounters many obstacles not present, or not as severe, for microsize particles (μPs). These difficulties are revealed in multiple experimental observations that are, unfortunately, not fully recognized as of yet. Inconsistencies in the accounting of NP interactions are observed across all material platforms that include ceramic, semiconductor, and metallic NPs; crystalline and amorphous NPs; as well as dispersions of inorganic, organic, and biological nanomaterials. Such systematic deviations of theoxretical predictions from reality point to the generality of such phenomena for nanoscale matter. Here we analyze the sources of these inconsistencies and chart a course for future research that might overcome these challenges.

ADVANCES: Nanoparticle interactions are often described by classical colloidal theories developed for μPs. However, several foundational assumptions of these theories, while tolerable for microscale dispersions, fail for NPs. For example, the sizes of ions, solvent molecules, and NPs can be within one order of magnitude of each other, which inherently disallows continuum approximations. Fluctuations of ionic atmospheres, ion-specific effects, enhanced NP anisometry, and multiscale collective effects become essential for accurate accounting of NP interactions. The nonuniformity of the stabilizing layer adds another essential contradistinction.

When the particle size becomes smaller than a few tens of nanometers and the gaps between particles become smaller than a few nanometers, nonadditivity of electrostatic (V_{el}), van der Waals (V_{vdW}), hydrophobic (V_{hph}), and other potentials (V') emerges. In fact, it becomes impossible to cleanly decompose the potential of mean force (PMF) for the interaction of two NPs into separate additive contributions from these interactions—as in, e.g., classical Derjaguin-Landau-Verwey-Overbeek (DLVO) theory [$V(r) = V_{el}(r) + V_{vdW}(r) + V_{hph}(r) + V'(r)$]—due to the coupled structural dynamics of neighboring NPs and surrounding media. Experimentally, the nonadditivity of NP interactions was observed long ago as an unusually high colloidal stability of NP dispersions, defying all reasonable predictions based on DLVO and other classical theories. It also manifests itself in paradoxical phase behavior, self-assembly into sophisticated superstructures, complex collective behavior, enigmatic toxicology, and protein-mimetic behavior of inorganic NPs. Molecular dynamics simulations of PMFs computed for NP pairs confirm the nonadditivity of van der Waals and electrostatic interactions for nanometer-scale separations.

OUTLOOK: Further work in the field of NP interactions should perhaps embrace NPs as strongly correlated reconfigurable systems with diverse physical elements and multiscale coupling processes, which will require new experimental and theoretical tools. Meanwhile, several heuristic rules identified in this Review can be helpful for discriminating between the systems in which mean-field theories can and cannot be applied. These precepts can guide qualitative thinking about NP interactions, stimulate further research into NP interactions, and aid in their design for applications.

ON OUR WEB SITE

Read the full article at http://dx.doi.org/10.1126/science.1242477

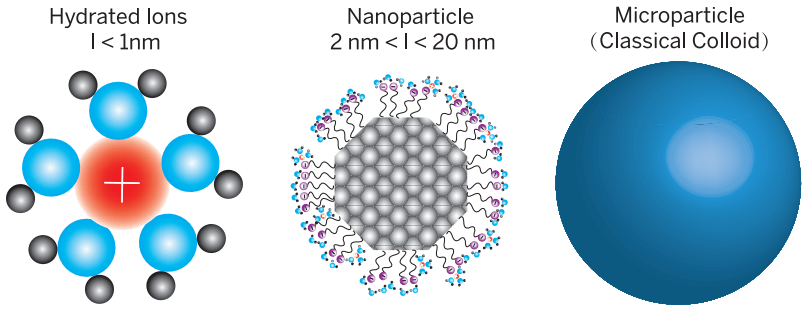

Schematics of hydrated ions, a NP, and a μP, demonstrating the structural uniqueness and discreteness of NPs. Nonadditivity of NP interactions stems from the size similarity of reconfigurable structural elements of NPs (i.e., surface ligands, ionic atmosphere, adsorbed molecules, etc.) and the surrounding media, leading to their strongly coupled dynamics. The high polarizability and faceting that are typical of NPs—as well as collective multibody effects at atomic, molecular, and nanometer scales—lead to the enhancement of nonadditivity and result in interdependence of electrostatic, van der Waals, hydrophobic, and other forces.

Though it is the crux of nonadditivity, the similarity in size between the ions and molecules composing the solvent medium and the NP offers a silver lining: it makes atomic simulations of their interactions increasingly practical as computer speed increases. The direct determination of the PMF by atomistic simulation bypasses the enumeration of individual forces and therefore resolves the nonadditivity problem. In fact, NPs present a favorable system for atomistic simulations because solid inorganic cores have many fewer degrees of freedom than flexible organic chains. Improvements in force fields are necessary to adequately account for intermolecular interactions, entropic contributions, dispersion interactions between atoms, high polarizability of inorganic materials, and quantum confinement effects.

Evolving experimental tools that can accurately examine interactions at the nanoscale should help to validate the simulations and stimulate improvement of relevant force fields. In fact, new opportunities for better understanding of the electronic origin of classical interactions are likely as the rapidly improving capabilities in synthesis, simulations, and imaging converge at the scale of NPs. ■

The list of author affiliations is available in the full article online.
*Corresponding author. E-mail: rlarson@umich.edu (R.G.L.); kotov@umich.edu (N.A.K.)
Cite this article as C. A. Silvera Batista *et al.*, *Science* **350**, 1242477 (2015). DOI: 10.1126/science.1242477

REVIEW

NANOPARTICLES

Nonadditivity of nanoparticle interactions

Carlos A. Silvera Batista,[1,2] Ronald G. Larson,[1,2,3]* Nicholas A. Kotov[1,2,3,4]*

Understanding interactions between inorganic nanoparticles (NPs) is central to comprehension of self-organization processes and a wide spectrum of physical, chemical, and biological phenomena. However, quantitative description of the interparticle forces is complicated by many obstacles that are not present, or not as severe, for microsize particles (μPs). Here we analyze the sources of these difficulties and chart a course for future research. Such difficulties can be traced to the increased importance of discreteness and fluctuations around NPs (relative to μPs) and to multiscale collective effects. Although these problems can be partially overcome by modifying classical theories for colloidal interactions, such an approach fails to manage the nonadditivity of electrostatic, van der Waals, hydrophobic, and other interactions at the nanoscale. Several heuristic rules identified here can be helpful for discriminating between additive and nonadditive nanoscale systems. Further work on NP interactions would benefit from embracing NPs as strongly correlated reconfigurable systems with diverse physical elements and multiscale coupling processes, which will require new experimental and theoretical tools. Meanwhile, the similarity between the size of medium constituents and NPs makes atomic simulations of their interactions increasingly practical. Evolving experimental tools can stimulate improvement of existing force fields. New scientific opportunities for a better understanding of the electronic origin of classical interactions are converging at the scale of NPs.

Over the past 20 years, there has been rapid progress toward the synthesis of nanoparticles (NPs) and the understanding of their distinct size- and shape-dependent physical phenomena. Preparation of NP dispersions has led to promising new materials for electronics, optics, energy storage, catalysis, medicine, and other technologies (*1*). Moreover, the ability of NPs to associate also leads to self-organization into superlattices (*2*–*5*) and supraparticular assemblies of varying dimensions (*6*, *7*). Multiparticle interactions are also responsible for the emergence of collective properties that are not present in individual NPs and encompass a wide spectrum of physical and chemical phenomena exemplified by Anderson excited states (*8*), multiparticle plasmonic resonances (*9*), collective Coulomb blockades (*10*), and others. Advancing these areas of knowledge and related technologies will require a detailed understanding of inter-NP interactions. Despite contributions from several disciplines and numerous authors, quantitative or even qualitative accounting of NP interactions is rarely achieved. The forces between NPs are largely the same as those between microsize particles (μPs). However, applying μP theories (*11*–*13*) and equations to NPs is problematic. The purpose of this Review is to (i) explain the source of these problems; (ii) organize diverse experimental, theoretical, and computational data into a consistent framework capable of describing interparticle interactions and assembly phenomena at the nanoscale; and (iii) chart a course for future studies that might overcome these obstacles.

[1]Department of Chemical Engineering, University of Michigan, Ann Arbor, MI 48109, USA. [2]Biointerfaces Institute, University of Michigan, Ann Arbor, MI 48109, USA. [3]Department of Biomedical Engineering, University of Michigan, Ann Arbor, MI 48109, USA. [4]Department of Materials Science and Engineering, University of Michigan, Ann Arbor, MI 48109, USA.
*Corresponding author. E-mail: rlarson@umich.edu (R.G.L.); kotov@umich.edu (N.A.K.)

What is a nanoparticle?

Within the framework of this Review, we define a NP as an inorganic particle, between 1 and 20 nm in diameter, together with a surrounding interfacial layer. The conclusions made for particles within this size range are valid for 100-nm particles that represent a commonly agreed dimensional threshold for nanoscale materials. However, the 1- to 20-nm size range provides the most vivid manifestations of quantum confinement, plasmonic effects, and other phenomena distinct to nanoscale materials. Yet the most severe problems in terms of agreement with theory tend to occur at this length scale, due to the convergence of the size of the constituents to within one order of magnitude of the particle size. Several characteristic distances describing interparticle interactions that fall into this range are discussed below.

We include the interfacial layer in the NP definition because measurements of properties of quantum dots, nanocrystals, nanowires, nanotubes, nanoplates, etc., all indicate that the interfacial layer is an integral part of nanoscale matter, fundamentally affecting its properties. The interfacial layer typically consists of organic molecules known as stabilizers, capping and surface ligands, or passivating agents. The inorganic part of the NPs (the core) is often (mono)crystalline; hence, the term "nanocrystal" is sometimes used interchangeably with "nanoparticle." Most of the considerations below are equally applicable to particles with cores that are not crystalline or polycrystalline, as long as they conform to the definition above. In fact, most, although not all, of the findings discussed in this paper are applicable to nanoscale particles of organic and/or biological materials (*14*, *15*). Here we will primarily focus on particles with inorganic cores.

Breakdown of common assumptions for particle interactions at the nanoscale

Both NPs and μPs are often similarly treated as classical colloids. Both types of particles often contain an inorganic core coated with a layer of surfactant (Fig. 1). Another commonality is that electrostatic and van der Waals (vdW) interactions are the two main forces between both μPs and NPs.

However, essential distinctions between NPs and μPs result from their size difference of one to five orders of magnitude (Fig. 1A). At least four key assumptions of classical theories, such as the Derjaguin-Landau-Verwey-Overbeek (DLVO) theory, are often valid at macro- and microdimensions but are no longer applicable when particles reach nanoscale size. The failures of the first two of these assumptions for NPs are the most difficult to overcome.

The first assumption is that solvent molecules and solvated ions are negligibly small compared with the dispersed particles. Contrary to such a model, the dimensions of the 1- to 20-nm NPs are comparable to the dimensions of solvent molecules, solvated ions, and other components of the solution, requiring consideration of the structural discreteness within the NPs and the surrounding medium.

The second assumption is that the total potential is a sum of multiple independent repulsive and attractive components (*12*, *16*)

$$V(r) = V_{el} + V_{vdW} + V' \quad (1)$$

where r is the center-to-center distance between the particles and V_{el}, V_{vdW}, and V' are distance-dependent potentials for electrostatic, vdW, and other interactions, respectively. Eq. 1 may also be referred to as the additivity assumption (*17*, *18*); it fails as the size of the particles and the distances between them reach nanoscale dimensions. NPs are often made from metals (such as gold, silver, platinum, nickel, and cobalt) or semiconductors (such as PbSe, PbS, and CdTe) with high polarizability that increases the coupling between different interactions, exacerbating the problem.

The third assumption is that the media outside and inside of the particle are uniform continua. Although this is related to the first assumption, it is treated separately in the original theories, which prompted us to keep these two assumptions distinct. Additionally, the first assumption refers primarily to the bulk state of the solvent, whereas the third assumption refers primarily to the interface between the NP and the surroundings. The breakdown of the third assumption for NPs is associated, among other

factors, with the interfacial layer, which has a thickness comparable to or sometimes even greater than the diameter of the NP cores. Thus, the thickness of the interfacial layer cannot be neglected, and both NPs and their surroundings can no longer be considered uniform continua. Another consequence of its breakdown is that the classical continuous dielectric function (ε) must be replaced with local atomic polarizability. By introducing image charges, advanced versions of DLVO and other colloidal theories can partially account for differences in ε between core, surface layer, and media. However, this approach also fails when the system displays molecular and nanoscale heterogeneity, including discreteness of ionic charge that cannot be ignored for NPs and their self-assembly processes (*19*).

The fourth assumption typical of the classical theory of colloids is that particles have simple shapes, typically spherical and less often cylindrical or ellipsoidal. The crystallinity of a NP core, on the other hand, leads to a great expansion of the palette of particle shapes: rods, dumbbells, cubes, hexagons, tetrahedrons, octahedrons, concave rhombic dodecahedra, tetrahexahedra, and others (Fig. 1, B to G) (*20*). Even NPs that are considered to be spherical are often actually prolate in shape, with an aspect ratio of 1.1 to 1.2 (*21*), and are also often faceted (*20*). Although the nonspherical shapes and interaction potentials can be incorporated into the classical colloidal theories, asymmetry of the shape may also originate from spontaneous unevenness of the surface layer, as was demonstrated for both gold and silica NPs (Figs. 1, B and C) (*22*, *23*). NPs with a thick stabilizer layer (Fig. 1A) can essentially change shape depending on the local environment. Such dynamic reconfiguration of particles is difficult to account for in the traditional models. Also, the presence of sharp apexes in tetrahedrons, pyramids, stars, and other particles creates singularity points that affect both the physics and chemistry of NPs. These singularity points are well known in plasmonics as so called "hot spots," but they are largely neglected in the consideration of intermolecular forces.

Although these assumptions are not always accurate for colloidal systems, many μP dispersions are lenient enough to neglect their failures, but the same is not true for NP dispersions.

Can DLVO theory be adapted to NPs?

The interactions between μPs are typically described by the DLVO theory. In its original formulation, DLVO theory considers only the two contributions V_{el} and V_{vdW} (*24*, *25*). The mean-field Poisson-Boltzmann (PB) formalism is typically used to obtain V_{el}, with the Debye-Hückel approximation yielding an analytical solution for small ionic strengths (I) not exceeding 0.01 M for 1:1 electrolytes and 0.0001 M for ions with high ion charge (z_i) (*12*). V_{vdW} is commonly calculated using the Hamaker theory (*26*) simplified by the Derjaguin approximation (*24*). This potential describes London dispersion interactions that are equated with vdW interactions within classical DLVO formalism. A potential of mean force (PMF) between two particles is calculated according to Eq. 1 as $V(r) = V_{el} + V_{vdW}$.

Over the past 50 years, much scientific work has been devoted to extending and improving DLVO theory to allow for more accurate equations for V_{el} and V_{vdW}, as well as wider ranges of I and z_i. Later versions of DLVO and the Sogami-Ise theory (*27*) give much improved predictions for counterions with $z_i > 1$, asymmetric electrolytes, and nonspherical particles. These theories may also include other types of interactions, allow a finite size of hydrated counterions, and account for discontinuities of the dielectric constant at interfaces (*28*, *29*). However, because of the conceptual problems noted above, even adaptations of many elegant theories developed for μPs are unlikely to have general applicability for NPs in the way that DLVO theory is applicable to microscale colloids. In particular, when particle size is reduced to the nanoscale, one needs to consider the finite size of solvated ions that are treated as point particles in DLVO theory and its many extensions. The diameters of common ions with their hydration shells encountered in NP dispersions are, for instance, 0.3 to 0.64, 0.45 to 0.47, 0.46 to 0.5, 0.40 to 0.6, 0.34 to 0.8, and 0.7 to 1.1 nm for Cl^-, Na^+, Cd^{2+}, Ca^{2+}, Mg^{2+}, and CO_3^{2-}, respectively (*30*–*32*); these values are comparable to the diameters of many small NPs. Moreover, two interacting NPs in typical assemblies often have a gap (d) as narrow as 1 to 2 nm between them (Fig. 1, D to G). Thus, even for the smallest ions and simplest interfacial layers, theoretical descriptions that ignore their finite dimensions cannot be applied to NPs.

When NP diameter reaches 1 nm, it also becomes comparable to or smaller than another characteristic distance—the Bjerrum length (l_B), which describes the separation at which the energy of electrostatic interactions between ions is equal to the thermal energy in the media, k_BT (k_B, Boltzmann constant; T, temperature). The PB and similar mean-field formalisms can be applied only when the charges are separated by distances much greater than l_B. This concept does not hold for the majority of interacting NPs (*1*–*7*, *11*, *13*, *14*, *33*, *34*) because l_B = 0.7 nm for aqueous media and 28 nm

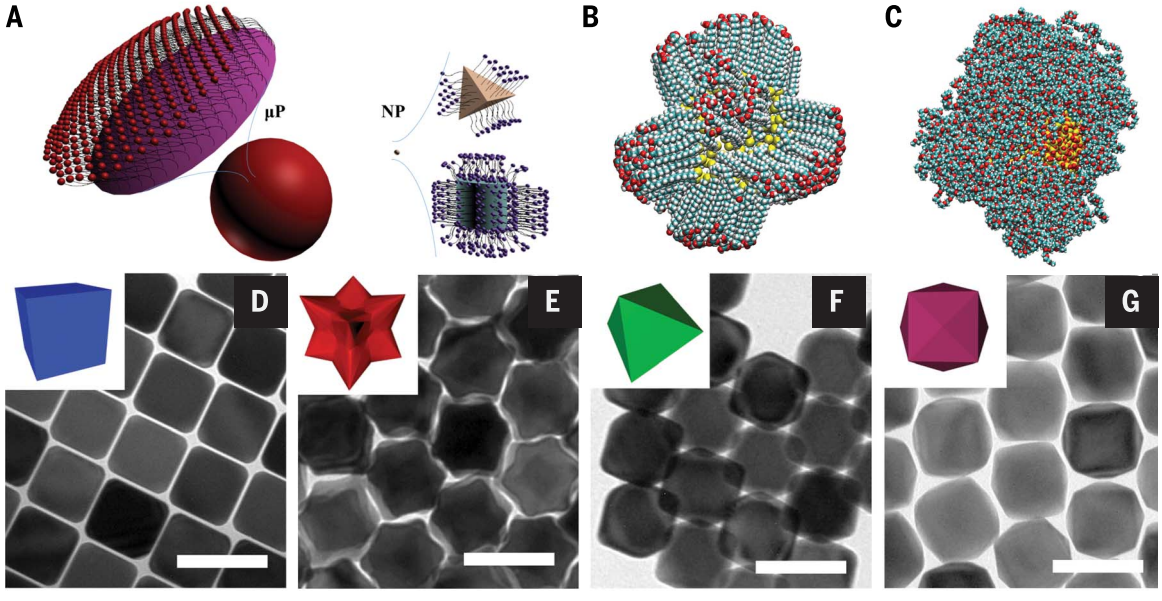

Fig. 1. Sizes and shapes of NPs. (**A**) Comparative pictorial representation of microscale and nanoscale particles. (**B** and **C**) MD simulations of 4-nm Au NPs coated with S–$(CH_2)_{17}$COOH (B) (*23*) and a 5-nm silica NP coated with (PEO)100 (C) (*22*). Yellow, sulfur; cyan, carbon; red, oxygen; blue, nitrogen; white, hydrogen. (**D** to **G**) Transmission electron microscopy (TEM) images of Au NPs with the shapes of cubes (D), concave rhombic dodecahedra (E), octahedra (F), and tetrahexahedra (G) obtained by seed-mediated oxidative-reductive growth cycles (*20*). Scale bars in (D) to (G), 100 nm.

for heptane. When the distances between charges become smaller than l_B, multiple ion-correlation effects (see below) occur, and this contradicts the central assumption of the Poisson distribution in the foundation of this theory.

One approach to adapting PB formalism for NPs would be to consider surface potential (ψ_0) as a variable dependent on r and other system parameters. However, for NPs, an adequate expression for $\psi_0(r,d,I,...)$ must account for the dynamic surface layer and therefore will require addressing the same issue of structural discreteness of the NP-solvent interface. In addition, surface layers often display variations in surface grafting density.

Even if the grafting density were completely uniform, the interaction potential between NPs would be nonspherically symmetric (Fig. 1, B and C), unlike the ordinary DLVO potential. The asymmetry of the potential is greatly enhanced when NPs are faceted or truncated (*35*, *36*).

An additional conceptual problem is that, when r and d are held constant, electrostatic and other potentials between the NPs fluctuate over time. Drastic fluctuations of V_{el} can be caused, for example, by single hydrated ions entering the interparticle space. These deviations cannot be described by typical colloidal-type potentials or steric repulsion (*37*, *38*).

Illustration of deviations

Several experimental studies have demonstrated that the DLVO theory can provide an adequate description for particles of 50 nm and larger (*39*, *40*). For example, modeling of plasmonic interactions has shown that the average distance between citrate-stabilized 80-nm Au NPs appears to correlate well with DLVO predictions (*41*). However, as the particles become smaller, deviations occur. As long ago as 1971 (*42*), it was noted that the classical treatment of interparticle forces incorrectly predicts that nanoscale silica should coagulate (*42*, *43*). Subsequent experimental (*44*–*47*) and computational (*48*) studies pointed out the unusual colloidal stability of NP dispersions under different media conditions. Contrary to the body of knowledge accumulated for μPs, a lack of a correlation was observed between the stability of NP dispersions and their charge or ionic strength—for instance, for 4-nm ZnO NPs (*49*) capped by humic acid or 2.3-nm Au NPs capped by mercaptoundecanoic acid (*50*). The deviations of the NP behavior were empirically rationalized by a specific packing of the interfacial layer, steric effects of the surface layer, preferential absorption of water at the NP interface, or incorporation of additional terms in Eq. 1, such as osmotic and elastic potentials (*45*, *51*, *52*). Thus, it is difficult to apply these principles to all NPs, and a different approach is needed.

Systematic behavioral deviations of NP dispersions are present across all material platforms. Even ligand-free Au NPs synthesized through laser ablation and stabilized by the tightly bound Stern layer of adsorbed ions were found to be stable against coagulation in the presence of F^- and SO_4^{2-}, whereas other anions with identical electrostatic valence, such as I^- and SCN^-, destabilize these suspensions (*47*).

Looking beyond dispersions, unusual behavior due to nonclassical NP interactions was also observed for phase transitions. In particular, octadecanethiol-capped 1.7-nm Au NPs reversibly recrystallize from an amorphous solid to a body-centered cubic superlattice upon heating (Fig. 2A). This is in contrast to the classical thermodynamics (*53*) expectation that recrystallization would occur upon cooling (*54*).

Deviations from classical behavior can also be consistently seen in atomistic molecular dynamics (MD) simulations of NPs. For instance, the size of a counterion strongly affects particle interactions, contrary to the DLVO predictions (*48*, *50*). As confirmed by experiments and simulations, a large counterion such as tetrabutylammonium hydroxide can provide a repulsive barrier, even at vanishing electrostatic potential (Fig. 2B). The presence of multiple extrema for 2-nm Au NPs revealed that the V_{el} displays a nonmonotonic dependence on interparticle center-to-center distance, contrary to predictions from PB formalism. Strong coupling of electrostatic, vdW, hydrophobic, and other forces accounts for this effect (Fig. 2C). Interparticle gaps $d < 2.5$ nm were found to be especially problematic, regardless of a specific NP diameter (*48*, *55*, *56*).

Substantial improvements in predictions of classical theories for ion concentration profiles may be achieved using classical liquid-state density functional theory (DFT) of the Carnahan-Starling type,

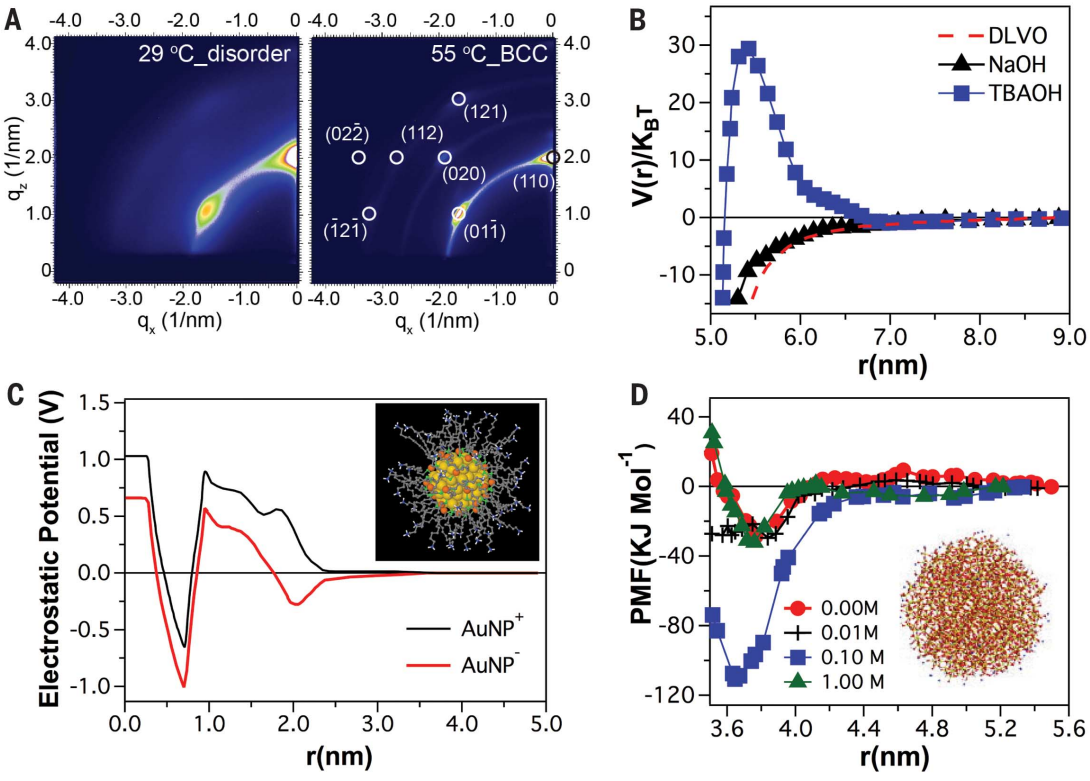

Fig. 2. Manifestation of nonadditivity of NP interactions in experiments and simulations. (**A**) Grazing-incidence small-angle x-ray scattering patterns for octadecanethiol-capped 1.7-nm Au NPs undergoing reverse phase transition (*53*). NP solids transform from disordered to crystalline upon heating from 29° to 55°C. (**B**) Comparison of the PMFs calculated according to DLVO (red) and MD simulations in the presence of positive ions of different diameters. Blue, tetrabutylammonium (TBA^+); black, Na^+. [Redrawn from (*48*)] (**C**) Radially integrated electrostatic potential in dispersions of 2 nm with different stabilizer layers: $Au_{144}(SR\text{-}NH_3^+)_{60}$ (black) and Au_{144} $(SR\text{-}COO^-)_{60}$ (red), where R is $\text{-}C_{11}H_{22}$. [Redrawn from (*56*)] (**D**) PMF for a pair of two amorphous 4.4-nm SiO_2 NPs in the presence of $[Na^+]$ = 0.00, 0.01, 0.10, and 1.00 M. [Redrawn from (*58*)] Insets in (C) and (D) show atomistic images of NPs used in the simulations. Notice that abscissas in (B) and (D) refer to the center-to-center interparticle distance (r) for spheres of 5.1- and 3.2-nm diameter, respectively.

even when the medium is described as a dielectric continuum. DFT models are able to capture the oscillatory density profiles of small ions and the charge inversion phenomena for uniformly charged 1.5-nm particles (*57*). As another example, PMFs for a pair of 4.4-nm silica NPs are similar in shape to that expected from the DLVO theory. However, these PMFs displayed maximum attraction and the deepest potential well for intermediate electrolyte concentration (Fig. 2D) (*58*) or multiple PMF extrema (Fig. 2C) (*56*), whereas DLVO theory predicts a monotonic decrease of repulsive electrostatic interactions (and, thus, the total energy of particle interaction) as I increases. More generally, it was found that for anionic NPs, DLVO theory overestimates $V_{el}(r)$ and underestimates it for cationic NPs. Also, the location of the attractive well is strongly shifted toward longer distances (*55*), which correlates well with the enhanced colloidal stability observed experimentally.

Self-organization phenomena at the nanoscale reveal even more clearly the limits of the predictive power of classical theories when applied to NPs. Formation of closely packed NP films, assemblies (*1*–*7*, *33*, *34*, *59*), and supraparticles (*60*) may be explained using hard-sphere, DLVO, or Yukawa-type PMFs. However, the differences between self-assembled structures found for μPs and NPs are particularly vivid because the close-range interactions make the errors of typical assumptions particularly influential. The entire spectrum of the crystal habits, including quasi-crystalline patterns, observed for NP superlattices cannot be explained by the classical PMFs (*34*). For instance, the inclusion of static dipolar interactions (i.e., Debye and Keesom forces) was found to be essential for explaining the packing of NPs into superlattices (*33*). The same is also true of NP assembly into chains, sheets, twisted ribbons, and shells (*6*, *7*, *36*, *61*, *62*), as well as for assemblies of NPs with other chemical species. When NPs are combined with proteins, multiple examples of discontinuities and counterintuitive trends are ascribed to "patchy" interactions (*63*–*66*). Many parallels in the behavior of NPs and globular proteins should also be noted (*15*, *67*, *68*). The strong influence of even subtle PMF asymmetry can also be seen in the enantioselective self-organization of chiral NPs (*62*).

Nonadditivity at the nanoscale

New experimental techniques to study forces applied to macroscale surfaces (*12*), microscale particles, molecules, and ions have been instrumental for appreciation of the complexity of interfacial forces at nanometer-scale separations. Nonadditivity of all major classes of interactions becomes apparent when analyzing the diverse sets of data at both single-particle and ensemble levels. Nonadditivity ultimately originates from the discreteness of matter that becomes dominant when distances become smaller than several tens of nanometers. As one of the manifestations of the nonadditivity, PMFs with multiple extrema stemming from the interdependence of vdW, electrostatic, and hydrophobic interactions are observed (Fig. 2). The unusual stability of dispersions of small NPs (*42*–*45*), numerous NP assemblies with extraordinarily sophisticated geometries, biomimetic behavior of NPs in their complexes with enzymes (*67*, *69*), and complex dynamics of protein coronas (*70*) represent experimental manifestations of nonadditivity.

The concept of interaction coupling is well known in molecular biology and is exemplified by ion-specific effects (ISEs) (*16*). More than a century ago, Franz Hofmeister recognized that ions with identical charge precipitate proteins to differing extents. It was later discovered that equally charged ions exhibit opposite tendencies to concentrate in the interfacial regions and can be classified by this tendency into chaotropes and kosmotropes. The Hofmeister series can be observed for many interfacial phenomena, usually when the Debye length is small. The order of ions in this series can be reversed when the polarity and/or the chemistry of the surface is changed.

Ion-specific effects stem from a complex set of nonadditive interactions between the ions, the solvent, and the surface; ISEs depend on the size, polarizability, and solvation of the ions, as well as on the hydrophobic or hydrophilic properties of the interface (*71*, *72*). The origin of ISEs may be simpler than it appeared at the time of Hofmeister. Due to discreteness of the matter at this scale, ions interact not only electrostatically but also via London dispersion interactions (*73*). At the first level of approximation and using the terms of the original theories, the potential of an ion within nanometers of the interface can be described as

$$V = V_{el} + V_{ISE}, \text{ where } V_{ISE} = V_{i\text{-}vdW} + V_{solv} + V_{image} \quad (2)$$

where V_{image} (*74*) and $V_{i\text{-}vdW}$ are image and van der Waals potentials, respectively, of ions near any surface, including that of NPs. As a simple demonstration of nonadditivity, $V_{i\text{-}vdW}$ is affected by the reorganization of the solvation shell and is therefore dependent on the solvation potential V_{solv} (*75*, *76*). Nonadditivity of ionic interactions translates into nonadditivity of interparticle forces, because V_{ISE} modifies the counterion distribution in the vicinity of the NP interface (*16*) and thus affects V_{el} and the other contributions to the PMFs of NPs (*71*, *73*). Although theoretical and simulation methods have been developed to describe ISEs (*73*, *77*), accounting for them accurately requires the simultaneous inclusion of hydration, ionic size, and polarizability effects, defying many theories. These effects become even more convoluted and escape direct theoretical quantification based on Eq. 2, especially for NP surfaces that display a mixture of polar and nonpolar groups.

The complexity of nanoscale electrostatics also manifests in ion-ion correlation (IIC) effects that originate from the discreteness or finite sizes of solvated ions and their mutual interactions (*78*). The latter are ignored in the mean field approximation that eventually leads to incorrect predictions of V_{el} (*79*), V_{solv}, and V_{image}. IICs are implicated in the peculiar behavior of μPs that is often described as charge inversion (*80*), charge amplification (*81*), and attraction of like-charged particles (*81*, *82*). Studies of these phenomena by atomic force microscopy (AFM) and optical tweezers have demonstrated that quantitative agreement with DLVO theory is possible for simple

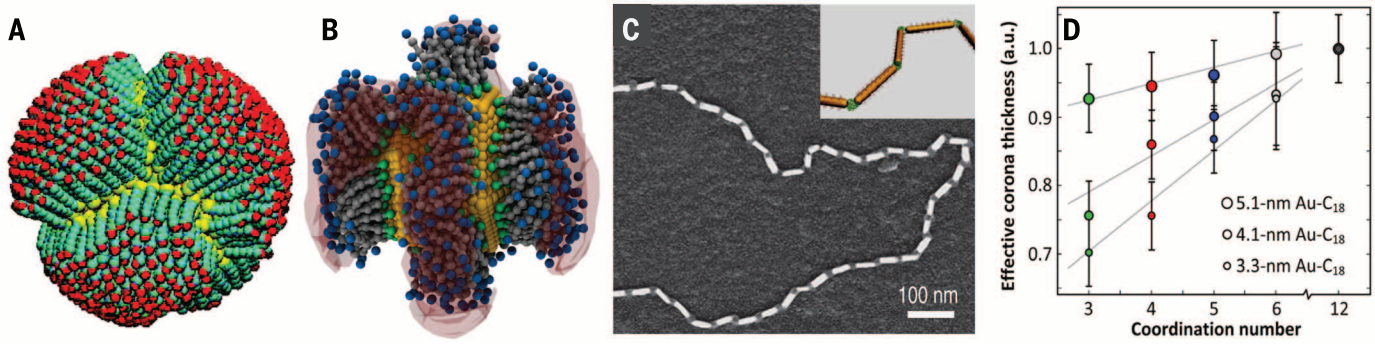

Fig. 3. Collective behavior of stabilizer molecules. (**A** and **B**) Snapshot of MD simulation of (A) spherical (*65*) and (B) icosahedral NPs (*109*) with charged groups at the core surface. For (B), isodensity surface of counterions and anions in the vicinity of the surface ligands is shown in pink. (**C**) Scanning electron microscopy image and schematic (inset) of the chains of end-modified gold nanorods (*120*). Scale bar, 100 nm. (**D**) Dependence of the effective thickness of the soft surface layer on the number of nearest neighbors in closely packed Au NPs (*112*). a.u., arbitrary units.

configurations of the individual μPs, but not for distances shorter than 5 nm (*46*), for multivalent ions (*83*), or for particles in the presence of additional surfaces (*82*), unless correction factors and additional interactions are incorporated.

The statistical mechanics of hard-sphere fluids has been an important theoretical tool in explaining these phenomena and has led to the development of several successful methods to describe IICs—namely, the liquid-state hypernetted chain (HNC) approximation, the Percus-Yevick approximation, and the mean spherical approximation. While providing a conceptual explanation for IIC phenomena, it was found that the effects of ionic size and Coulombic interactions are interdependent and that computational results defy expectations based on additivity of constitutive potentials (*84*, *85*).

Ion-ion correlations are relevant within several ionic diameters (*85*) and a length scale of ~$3.6\lambda_{GC}$, where λ_{GC} is the thickness of the Gouy-Chapman layer (*86*, *87*) of counterions (~2 to 4 nm) (*88*). At distances much larger than λ_{GC} (i.e., 20 to 100 nm), the IICs are weak and the distribution of ions can be described fairly accurately by the PB equation, which is consistent with the AFM experiments using latex μPs (*88*) and the quantitative theoretical account of IIC using the Yvon-Born-Green hierarchy (*89*).

Besides correlated dynamics of ions, excluded volume effects arising from the finite volume of ions make a large contribution to IICs. Hence, the ion density distributions do not monotonically decrease with distance from the surface but rather become oscillatory, reflecting the dimensions and molecular identity of solvated ions (*78*). Such oscillations can extend for distances of up to $14.5l_B$ (*87*) or, by other estimates, 15 nm (*85*).

Ion-ion correlations are especially important for charged NPs for which electrostatic interactions between ions become much larger than the thermal energy. Thus, the counterion cloud behaves as a strongly correlated liquid. In nanocolloids, IICs may lead to an apparent attractive nanoscale-range interaction that is comparable in strength to vdW interactions and that increases in strength with NP charge (*87*).

Alteration of the structure of water around interfaces and solutes gives rise to intermolecular interactions, commonly known as hydrophobic interactions. Their potential, V_{hph}, is nonadditive with V_{el} and V_{vdW} (*17*). Molecular disturbances, which are essential for understanding hydrophobic interactions, were observed around NPs for distances of up to 2 nm for a variety of solvents—e.g., water (*90*), propanol, and ethanol (*91*). Similar ranges exceeding 1 nm were observed in MD simulations for C_{60} buckminsterfullerene and 2-nm Au NPs (*92*). Terahertz spectroscopy that directly probes solvation dynamics revealed the width of the dynamical hydration layer around proteins to be 2 nm as well (*93*).

Historically, hydrophobic interaction has been attributed to the reduction in entropy of liquid water upon solubilization of nonpolar molecules due to the formation of a rigid icelike cage by the water molecules around the solutes. More recently, however, simulation (*94*) and Raman scattering experiments (*95*) have demonstrated that this mechanism is valid only for small solutes. A transition from a structured hydration shell to a "dry" disordered shell with lower water density takes place when the solute reaches a size of ~1 nm (*94*). The interface of this dry disordered shell is formed by water molecules having "dangling" -OH groups with broken hydrogen bonds (*96*), and enthalpy rather than entropy dominates the free energy of solvation. Thus, for large solutes, both hydrogen bonds and dispersion interactions between solutes and solvents make contributions to the balance of solvation energies.

Because electrostatic interactions can alter the organization of water at the interfaces, hydrophobic interactions become intrinsically dependent on the charge state of the interface and on the presence of ions in its vicinity. Therefore, these interactions are intertwined with electrostatic forces (*97*). Moreover, charge nonuniformity on a scale comparable to that of hydrophobic forces increases the interdependence of V_{el} and V_{hph}. Dynamic charge variations can stem from the stochastic distribution of ions and electrons and from local chemistry.

Initially, the coupling of hydrophobic forces with other interactions was suspected from simulations of proteins with hydrophobic patches (*98*). Very recently, chemical AFM measurements revealed a dramatic change in the strength of hydrophobic interaction on co-immobilization of amine or guanidine residues. These residues are surrounded by a different water shell; protonation of amine groups doubles the strength of hydrophobic interactions, whereas guanidinium groups eliminate measurable hydrophobic interactions in all of the pH ranges investigated (*17*).

Atomic multibody polarization effects are the key reason for the nonadditivity of the London dispersion forces. Their nonadditivity reflects the fact that the polarizability of an atom is affected by the dynamic polarization state of adjacent atoms and includes collective components of polarizability (*99*). In other words, integration of dispersion interactions between pairs of atomic voxels, assuming their independence, introduces large errors when used to assess the attraction of particles of nanoscale dimensions. For small molecules or relatively large particles with dimensions of several tens of nanometers, the errors do not exceed 10 to 15% (*100*). Conversely, the additive calculations using the Derjaguin approximation were shown

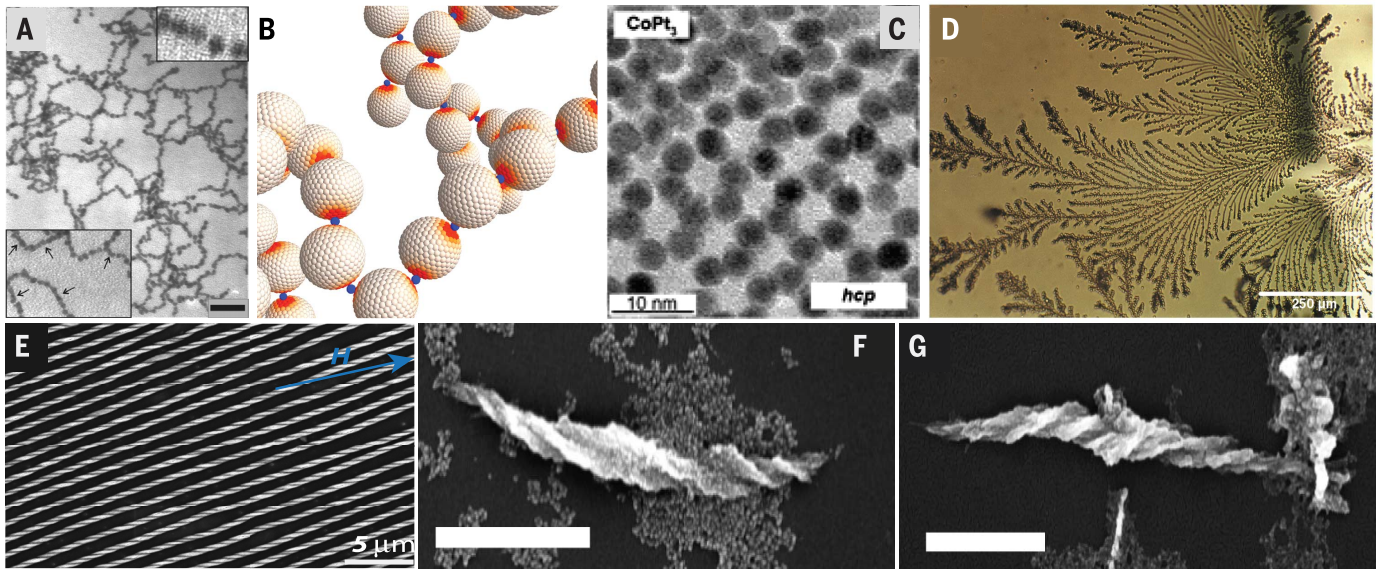

Fig. 4. Nonadditivity effects in self-organization of NPs. (**A**) Assembly of CdTe NPs in branched chains (*6*). Scale bar, 50 nm. (**B**) Simulated assemblies with multibody effects due to polarization (*19*). (**C**) One-layer superlattice from $CoPt_3$ NPs (*33*). (**D**) Dielectrophoretic assembly of dendrites from 15- to 30-nm Au NPs (*127*). (**E**) Assembly of ~10-nm cubic magnetite NPs with helical packing as the result of the interplay between magnetic dipole coupling and close packing (*128*). (**F** and **G**) Enantioselective assemblies of chiral CdTe NPs into left- and right-winded helixes (*62*). Scale bars in (F) and (G) are 150 nm.

to produce large errors for particles ~16 nm in diameter (*101*). Theoretical studies have shown that the interaction energy between small NPs asymptotes to the pairwise sum when the interparticle separation reaches about one particle diameter, and it deviates by 17% when the NPs are in near contact (*102*). However, in some cases the classical pairwise description is sufficiently accurate because the higher-order terms cancel each other (*103*). Such compensation occurs most often for isotropic bodies and is strongly dependent on geometry and separation distances between them. MD simulations for 1- to 5-nm silicon NPs (*104*) using the COMPASS force field yielded values of both attractive London dispersion and repulsive close-range Born forces that differed by several orders of magnitude from results based on their pairwise additivity.

The largest deviations are expected for highly polarizable (plasmonic) materials (*105*). The contribution of multibody effects doubles the attractive forces over those calculated by Hamaker theory for NPs in this case (*102*). The importance of nanoscale effects on dispersive interactions is further enhanced by size-dependent quantum confinement effects (*106*) and bond length variability (*107*) affecting the polarizability of atoms and particles.

A particularly vivid example of nonadditivity can be observed in the collective behavior of stabilizer ligands on a NP surface, representing multibody phenomena at molecular scale in NPs (Fig. 3). The collective behavior of surface ligands is the direct consequence of the multiplicity of interdependent molecular processes: grafting layer transitions, stabilizer entropy, faceting, solvent structuring, hydrogen bonding, hydrophobic interactions, and electrostatic repulsion of the charged groups at the solvent-ligand interface. In such a system, a change in the electrostatic component does not occur separately from the other interactions. Therefore, no sum of individually defined potentials can describe the interactions of such particles at distances comparable to NP diameters and ligand lengths, such as interparticle gaps of a few nanometers.

Spontaneous bunching of ligands is an illustration of collective behavior in surface layers of NPs (Fig. 3A) (*65*). Surface phase separation patterns can appear for chemically distinct stabilizers, as well as for surface ligands of different lengths that maximize the entropy of their head groups by surface segregation (*108*). The oligomeric character of the ligands and the solvent facilitates such behavior (*35*, *37*, *102*); faceting of the NPs can further enhance it as well (Fig. 3B) (*35*, *109*), resulting in a 100× increase in both association constants and rates of NP aggregation (*110*).

The dynamic restructuring of the surface layer on NPs in close contact results in a considerable attractive force due to both entropic (*111*, *112*) and entalpic effects. The former are related to the tendency of the ligands to maximize their degrees of freedom. Besides the variety of intermolecular interactions mentioned above, the latter ones can also originate from fluctuations of the ligands (*38*), analogous to the London dispersion force. Based on MD simulations, the London-like interactions from dynamic reconfiguration of the surface layer may contribute as much as $6k_BT$ to the total interaction potential (*113*). Interparticle forces at the nanoscale can, in fact, be dominated by collective ligand alignment that organizes nearby solvent molecules (*114*).

Together, the multibody effects in surface layers lead to Dzugutov-like (*115*) and more complex potentials (Fig. 2C) that, in turn, result in notable macroscopic effects exemplified by unexpected rotatory optical activity of dispersions (*21*), reverse temperature transition (Fig. 2A) (*53*), and formation of superlattices with complex periodicities (*116*) such as quasi-crystals (*117*, *118*).

Nonspherically symmetric interactions owing to uneven ligand densities also play a role (*119*). Collective restructuring of the oligomers coating NPs maximizing hydrophobic interactions is implicated in the formation of chains of end-modified gold nanorods (*120*) and hexagonally packed mesoscale capsules (Fig. 3C) (*121*). Reconstruction and compressibility of the stabilizer layer on particle-particle contact strongly affect the effective NP diameter (Fig. 3D). This reconstruction typically increases the "stickiness" of NPs, promoting formation of amorphous solids (*122*, *123*).

Multibody effects of NPs manifest themselves particularly vividly in large ensembles of interacting particles (*124*). Entropic effects can make an essential contribution for such NP systems. In a simple case of hard particles with PMFs containing only short-range repulsion and no attraction, the collective maximization of degrees of freedom of faceted particles similar to those in Fig. 1 results in their ordering into a variety of crystalline and quasi-crystalline superlattices (*125*). For more complex PMFs corresponding to dispersions, the rotational, translational, or vibrational motions of NPs become coupled with the entropy of solvent molecules, ions, and stabilizer molecules.

Collective behavior of NPs also reflects orientational preferences of NP association and angular anisotropy of PMFs. Anisotropy of interactions between individual NPs manifests particularly well in large NP ensembles; can be driven by internal or external electrostatic or magnetic fields; and can lead to NP self-organization into chains (Fig. 4, A and B), superlattices (Fig. 4C), or dendrites (Fig. 4D) (*126*, *127*) and potentially many other extended assemblies. The collective behavior of NPs amplifies the effect of seemingly small energetic contributions to PMFs. For instance, static and dynamic dipolar polarization in the ground state of NPs is generally neglected but is capable of guiding the association into several common assembly patterns (*6*, *7*, *19*, *61*). Evidence that weak interactions are capable of having large effects on the geometry of NP assemblies can also be observed in the formation of helical superstructures (Fig. 4, E to G) (*61*, *62*, *128*) from chiral (*62*) and nonchiral (*128*) NPs.

Heuristic rules

Heuristic rules can guide qualitative thinking about NP interactions, whereas quantitative understanding will require new theoretical and computational approaches, which we discuss next. Heuristic rules could be helpful for discriminating between the systems where PB, DLVO, and other mean-field theories can and cannot be applied to NP interactions. Although this study indicates that universal laws regarding NP interactions are currently hard to come by due to diversity of mechanisms and scales of nonadditivity, the following trends emerge:

1) The use of PB theory for point charges is only reasonable for ion diameters that are less than 10% of NP diameter. For ions larger than this, liquid-state theory, involving the HNC or other approximations, becomes more useful.

2) Small ligands such as citrate ions might be considered simple stabilizers that do not respond to neighboring particles; when the stabilizer length becomes comparable to the NP diameter, the surface layer responds strongly to neighboring particles, producing large nonadditive interactions.

3) Solvent molecules with a characteristic length scale of 1 nm enhance nonadditivity of NP interactions (*17*, *94*, *95*).

4) Dynamic correlations between charged NPs become important when the electrostatic energy between them becomes comparable to k_BT.

5) The empirical Hofmeister series can provide guidance in predicting ion-specific effects in NP interactions (*15*). These expectations are confirmed by recent data (*47*, *129*, *130*).

6) Higher polarizability of the NP core must lead to stronger nonadditivity effects. This rule originates from the increase of the reconfigurability scale for electron density in NPs in response to external stimuli. It can be compared to the enhancement of non-DLVO behavior of polarizable ions (*72*). This rule manifested in theoretical studies of vdW interactions for NPs (*103*, *131*).

These practical rules of thumb should help facilitate further research into NP interactions and aid molecular design of NPs for applications. In perspective, the multiplicity of nonadditivity mechanisms indicates that further conceptualization and theoretical development of this field must involve a new way of thinking about NPs as strongly correlated reconfigurable systems with diverse physical elements and multiscale coupling processes.

Atomistic potential of mean force for NP interactions

Besides highlighting the distinct issues and general regularities associated with NP interactions, we also want to begin answering the question of how to adequately treat the complex mutually correlated forces between NPs. Because of nonadditivity, all interactions must be considered simultaneously. Because of discreteness of matter at a scale relevant to NP interactions, molecular- and atomic-scale phenomena cannot be averaged out. In other words, a reasonable correlation with experiment cannot be expected by adding smooth potentials for electrostatic, dispersive, hydrophobic, magnetic, and other interactions individually corrected for nanoscale effects. Fortunately, molecular simulation methods, which can address both discreteness and nonadditivity, have reached impressive levels of speed and reliability.

The reduced dimensions of the nanoscale and the corresponding reduction in numbers of atomic degrees of freedom become a distinct advantage when simulating NPs with atomistic resolution. Also, advances in electron microscopy afford accurate visualization of the three-dimensional (3D) geometry of NPs, allowing the possibility of direct validation of molecular simulations. In fact, we are now at a juncture at which the accuracy of synthesis, the length and time scales of molecular simulation, and the imaging capabilities all overlap at the "sweet spot" of NP dimensions.

Thus, a rational strategy for future progress in the understanding of NP interactions is to use these capabilities to bypass enumeration of individual forces and to determine the net interparticle PMF directly from atomistic simulations. This strategy enables adequate accounting for nonadditivity of interactions at the nanoscale, exemplified by the difficulties of incorporation of ISE, IIC, and hydrophobic potentials as independent terms in, for instance, Eq. 1. Hydrogen bonding, capillary action, and other forces that may contribute to self-organization of NPs (*1*, *11*, *13*, *62*) can be included with this method as well. Simulated PMFs can be verified by predicting the stability of nanocolloids and NP self-assembly patterns. In some cases of larger particles, additional verification can be obtained by taking advantage of liquid-cell electron microscopy techniques (Fig. 5, A and B) and extracting the PMF directly from NP diffusion (*132*).

Although the calculation of PMFs directly from molecular simulation remains in its infancy, recent work indicates that this strategy is viable. An example is the MD simulation of the PMFs of CdS nanorods stabilized by octadecyl thiol in *n*-hexane (Fig. 5, C and D) (*114*). Unlike the Hamaker theory, the simulations capture the complex interplay of the dispersion forces between the inorganic rods, the collective behavior of surface ligands, and the ordering of solvent molecules, providing a detailed picture of interactions between the nanoscale particles (*133*). The progressive changes in physical properties with varying particle sizes (1 to 4 nm) of metal (*133*, *134*) and semiconductor NPs (*135*) containing as many as 8217 atoms can also be realistically described by the MD technique.

Despite shared force-field problems with biomolecules, NPs present a favorable system for atomistic simulations as compared with proteins and polymers. Solid inorganic cores have many fewer degrees of freedom than flexible organic chains, making NPs more realistic for MD, Monte Carlo (MC), and other simulation algorithms with limited computer power.

Considering the emerging possibility of an MD-PMF strategy for nanoscale systems, several important challenges must be mentioned. One challenge is the lack of sufficient computer power to run large simulations with atomistic resolution. This limitation is particularly notable when one needs to incorporate quantum calculations with MD code. These calculations are needed to adequately describe interactions of atoms in the NP core and surface ligands.

Although the computer power limitation fades with each passing month, there are several other caveats. MD simulations have been used extensively in structural biology to resolve similar difficulties originating from the nonadditivity of nanoscale interactions and dynamics of proteins, DNA chains, lipid membranes, etc. Their success, however, has been limited because the existing MD force fields inaccurately describe many intermolecular interactions, especially hydrogen bonds. Second, the difficulties with including entropic contributions of the chemical groups and hydrophobic interactions should also be noted. Third, dispersion interactions between atoms are usually described in MD codes by pairwise summation of atomic Lennard-Jones potentials that ignore the polarization multibody effects. Last, the pairwise PMF neglects higher-order multibody effects that arise from influences of other particles on the particle pair and vice versa. So, the development of a PMF via simulation, while accounting for the nonadditivity of electrostatic, dispersive, and other forces between two NPs, proceeds by assuming additivity of interactions at the atomic scale and still leaves the assumption of nonadditive interactions among multiple NPs. Thus, traditional atomistic simulations are not a panacea but must be augmented by improved force fields and additional computational tools to address remaining issues of nonadditivity.

The existing MD force fields were developed and optimized for organic and biological molecules. They are suitable to describe the collective behavior of stabilizer ligands on a NP surface. However, force fields optimized for inorganic NPs are a rarity (*135*). Going forward, improvements in MD force fields need to be made while accounting for the specifics of NP interactions. As such, they should include a more adequate account of the nonadditivity of dispersion interactions. The Dzyaloshinskii-Lifshitz-Pitaevskii (DLP) theory (*136*, *137*) and the coupled-dipole method (CDM) (*99*, *102*) are currently the most promising approaches for evaluating dispersion forces. Nevertheless, both DLP theory and CDM are rarely used outside of the realm of theoretical physics, with a few exceptions involving μPs or NPs as noted below.

Continuum DLP theory (*28*) accounts for multibody effects, complex electrodynamics of atomic ensembles in the presence of an intervening medium, and retardation of electromagnetic waves through the use of dielectric function determined either experimentally (*138*) or computationally (*139*). The application of DLP to NPs has been limited, but a few studies demonstrate a strong mismatch between dispersion forces calculated with and without polarization multibody effects, especially for organic solvents (*140*) and small particles of few-nanometer size (*141*). The limitation of DLP theory is that the molecular and atomic details of the particle's interface are smeared out, which inhibits its ability to account for facets, apexes, or edges. This theory will also have

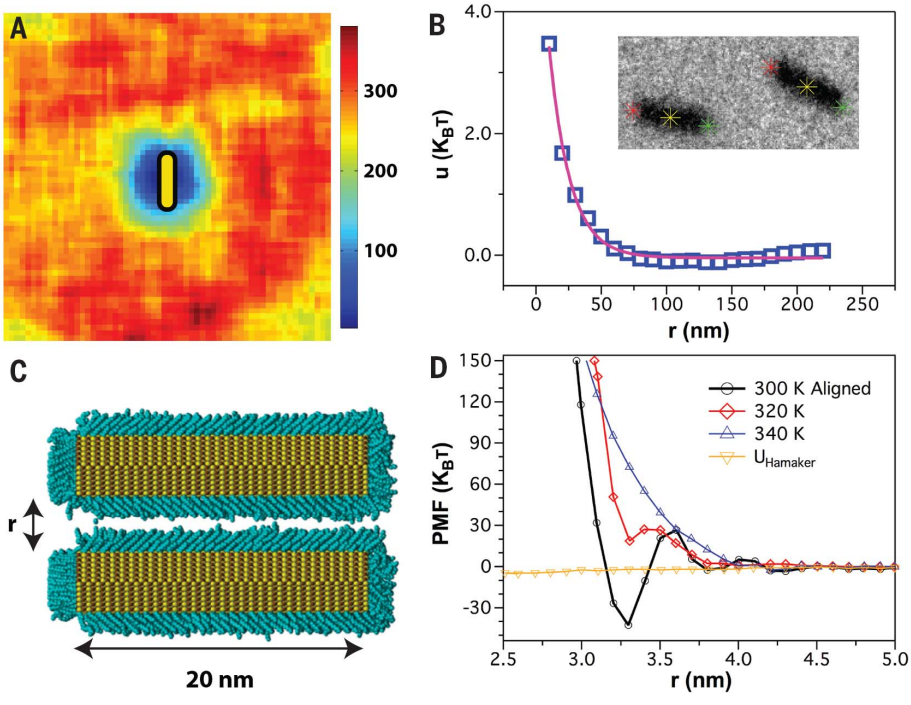

Fig. 5. Experimental and computational methods to obtain potential of mean force. (**A**) Color-coded counts of the total number of rods in the 2D plane pixels obtained by the real-time monitoring of nanorod behavior in liquid by TEM (*132*). (**B**) Experimental PMF for Au nanorods (inset) obtained by TEM imaging in liquid cells. (**C**) CdS 4-nm–by–20-nm faceted nanorods coated with alkyl thiol molecules and (**D**) their simulated PMFs at the temperatures indicated in *n*-hexane, where *r* is the distance between the opposing crystal facets (*114*).

difficulties accounting for NP surface dynamics that is essential at close separations.

The coupled-dipole method represents a fluctuation-based approach, similar to DLP, but remains valid when a continuum description of the NPs is not applicable. CDM views atoms individually as simple harmonic oscillators. Simultaneously, coupling of oscillators (i.e., atomistic multibody interactions) is allowed, thus avoiding atomic-level pairwise additivity. Because finding eigenvalues (frequencies) of this large system of coupled atomic oscillators is essential for CDM, its size represents one of the limiting factors for this approach, which we believe can be successfully resolved, even with current codes and computational hardware. The polarizability of atoms is usually described by the Drude model, but it often results in the so-called "polarizability catastrophe" for closely spaced atoms. Future improvements of CDM should include ab initio methods to calculate atomic polarizability, such as time-dependent DFT (*142*, *143*), that can also incorporate retardation effects. Integration of quantum mechanics with CDM would make it possible to discriminate the electronic characteristics of atoms located in different parts of NPs (*144*). Validation of the different options for quantum mechanics–enhanced CDM models can be made using the well-established properties of individual NPs.

It also will be important to develop MD force fields that account for quantum confinement effects, as well as the diversity and specificity of atomic arrangements in NPs. Although there are numerous examples of successfully using quantum mechanics to calculate atomic charges, such methods are applicable only to relatively small atomic systems. Similar issues arise in any attempt to integrate CDM-based algorithms into MD simulations. In particular, the dynamics of the solvent and ions around NPs will require recalculation of parameters for dipolar coupling in every MD step due to time-varying interatomic distances. The computational costs for such a method could perhaps be reduced by using CDM on small subsystems to tune or "train" MD parameter sets specifically for each system, before a regular MD simulation.

Because computer speed is constantly increasing, we shall arrive at fairly accurate calculations of pairwise PMFs of NPs at some point in the future. The effects of NP material, size, ligand coating, and ions on NP interactions can then be systematically studied and, if necessary, deconvoluted. Then, pairwise additivity at the level of NP-NP interactions will need to be tested and multibody corrections made, which will be particularly essential for understanding the self-assembly phenomena. Testing the results of such simulations is increasingly made possible by experimental advances such as liquid-cell electron microscopy. Large ensembles of NPs would be best described by transitioning to coarse-grained models (*125*, *145*). Besides MD, MC, dissipative particle dynamics, and other algorithms could be used at this point, depending on the scientific question. Some of them have already been used for μPs and NPs after PMFs were determined. Coarse-grained models have demonstrated an ability to describe systems containing many thousands of particles, which is large enough to reach micrometer-scale dimensions. Simulations at this scale can be tested by many other experimental methods, including traditional optical microscopy, to verify coarse-grained models and observe temporal transformations. Thus, despite the challenges, there is reason for optimism that exciting progress in understanding, predicting, and exploiting the distinct properties of NP assemblies is on the horizon.

REFERENCES AND NOTES

1. Z. Nie, A. Petukhova, E. Kumacheva, Properties and emerging applications of self-assembled structures made from inorganic nanoparticles. *Nat. Nanotechnol.* **5**, 15–25 (2010). doi: 10.1038/nnano.2009.453; pmid: 20032986
2. N. A. Kotov, F. C. Meldrum, C. Wu, J. H. Fendler, Monoparticulate layer and Langmuir-Blodgett-type multiparticulate layers of size-quantized cadmium sulfide clusters: A colloid-chemical approach to superlattice construction. *J. Phys. Chem.* **98**, 2735–2738 (1994). doi: 10.1021/j100062a006
3. C. B. Murray, C. R. Kagan, M. G. Bawendi, Self-organization of CdSe nanocrystallites into three-dimensional quantum dot superlattices. *Science* **270**, 1335–1338 (1995). doi: 10.1126/science.270.5240.1335
4. L. Motte, F. Billoudet, E. Lacaze, M.-P. Pileni, Self-organization of size-selected, nanoparticles into three-dimensional superlattices. *Adv. Mater.* **8**, 1018–1020 (1996). doi: 10.1002/adma.19960081218
5. M. Li, H. Schnablegger, S. Mann, Coupled synthesis and self-assembly of nanoparticles to give structures with controlled organization. *Nature* **402**, 393–395 (1999). doi: 10.1038/46509
6. Z. Tang, N. A. Kotov, M. Giersig, Spontaneous organization of single CdTe nanoparticles into luminescent nanowires. *Science* **297**, 237–240 (2002). doi: 10.1126/science.1072086; pmid: 12114622
7. Z. Tang, Z. Zhang, Y. Wang, S. C. Glotzer, N. A. Kotov, Self-assembly of CdTe nanocrystals into free-floating sheets. *Science* **314**, 274–278 (2006). doi: 10.1126/science.1128045; pmid: 17038616
8. M. V. Artemyev, A. I. Bibik, L. I. Gurinovich, S. V. Gaponenko, U. Woggon, Evolution from individual to collective electron states in a dense quantum dot ensemble. *Phys. Rev. B* **60**, 1504–1506 (1999). doi: 10.1103/PhysRevB.60.1504
9. M. Hentschel *et al*., Transition from isolated to collective modes in plasmonic oligomers. *Nano Lett.* **10**, 2721–2726 (2010). doi: 10.1021/nl101938p; pmid: 20586409
10. C. A. Stafford, S. Das Sarma, Collective Coulomb blockade in an array of quantum dots: A Mott-Hubbard approach. *Phys. Rev. Lett.* **72**, 3590–3593 (1994). doi: 10.1103/PhysRevLett.72.3590; pmid: 10056238
11. Y. Min, M. Akbulut, K. Kristiansen, Y. Golan, J. Israelachvili, The role of interparticle and external forces in nanoparticle assembly. *Nat. Mater.* **7**, 527–538 (2008). doi: 10.1038/nmat2206
12. J. Israelachvili, *Intermolecular and Surface Forces* (Academic Press, London, ed. 3, 2011).
13. K. J. M. Bishop, C. E. Wilmer, S. Soh, B. A. Grzybowski, Nanoscale forces and their uses in self-assembly. *Small* **5**, 1600–1630 (2009). doi: 10.1002/smll.200900358; pmid: 19517482
14. V. Dahirel, M. Jardat, Effective interactions between charged nanoparticles in water: What is left from the DLVO theory? *Curr. Opin. Colloid Interface Sci.* **15**, 2–7 (2010). doi: 10.1016/j.cocis.2009.05.006
15. N. A. Kotov, Chemistry. Inorganic nanoparticles as protein mimics. *Science* **330**, 188–189 (2010). doi: 10.1126/science.1190094; pmid: 20929766
16. M. Boström, D. R. Williams, B. W. Ninham, Specific ion effects: Why DLVO theory fails for biology and colloid systems. *Phys. Rev. Lett.* **87**, 168103–168106 (2001). doi: 10.1103/PhysRevLett.87.168103; pmid: 11690249
17. C. D. Ma, C. Wang, C. Acevedo-Vélez, S. H. Gellman, N. L. Abbott, Modulation of hydrophobic interactions by proximally immobilized ions. *Nature* **517**, 347–350 (2015). doi: 10.1038/nature14018; pmid: 25592540
18. B. W. Kwaadgras, M. W. J. Verdult, M. Dijkstra, R. van Roij, Can nonadditive dispersion forces explain chain formation of nanoparticles? *J. Chem. Phys.* **138**, 104308 (2013). pmid: 23514490
19. K. Barros, E. Luijten, Dielectric effects in the self-assembly of binary colloidal aggregates. *Phys. Rev. Lett.* **113**, 017801–017806 (2014). doi: 10.1103/PhysRevLett.113.017801; pmid: 25032932
20. M. N. O'Brien, M. R. Jones, K. A. Brown, C. A. Mirkin, Universal noble metal nanoparticle seeds realized through iterative reductive growth and oxidative dissolution reactions. *J. Am. Chem. Soc.* **136**, 7603–7606 (2014). doi: 10.1021/ja503509k; pmid: 24830921
21. X. Wu *et al*., Unexpected chirality of nanoparticle dimers and ultrasensitive chiroplasmonic bioanalysis. *J. Am. Chem. Soc.* **135**, 18629–18636 (2013). doi: 10.1021/ja4095445; pmid: 24246036
22. K. M. Salerno, A. E. Ismail, J. M. D. Lane, G. S. Grest, Coating thickness and coverage effects on the forces between silica nanoparticles in water. *J. Chem. Phys.* **140**, 194904 (2014). doi: 10.1063/1.4874638; pmid: 24852560
23. D. S. Bolintineanu, J. M. D. Lane, G. S. Grest, Effects of functional groups and ionization on the structure of alkanethiol-coated gold nanoparticles. *Langmuir* **30**, 11075–11085 (2014). doi: 10.1021/la502795z;pmid: 25162679
24. B. V. Derjaguin, L. Landau, Theory of the stability of strongly charged lyophobic sols and of the adhesion of strongly charged particles in solutions of electrolytes. *Acta Phys. Chem. URSS* **14**, 633–662 (1941).
25. T. J. Verwey, E. J. W. Overbeek, K. Van Ness, *Theory of the Stability of Lyophobic Colloids: The Interactions of Sol Particles Having an Electric Double Layer* (Elsevier, New York, 1948).
26. H. C. Hamaker, The London—van der Waals attraction between spherical particles. *Physica* **4**, 1058–1072 (1937). doi: 10.1016/S0031-8914(37)80203-7
27. I. Sogami, N. Ise, On the electrostatic interaction in macroionic solutions. *J. Chem. Phys.* **81**, 6320 (1984). doi: 10.1063/1.447541
28. I. E. Dzyaloshinskii, E. M. Lifshitz, L. P. Pitaevskii, General theory of van der Waals' forces. *Sov. Phys. Usp.* **4**, 153–176 (1961). doi: 10.1070/PU1961v004n02ABEH003330
29. V. A. Parsegian, B. W. Ninham, Van der Waals forces in many-layered structures: Generalizations of the Lifshitz result for two semi-infinite media. *J. Theor. Biol.* **38**, 101–109 (1973). doi: 10.1016/0022-5193(73)90227-0; pmid: 4707770
30. J. Kielland, Individual activity coefficients of ions in aqueous solutions. *J. Am. Chem. Soc.* **59**, 1675–1678 (1937). doi: 10.1021/ja01288a032
31. Y. Marcus, Ionic radii in aqueous solutions. *Chem. Rev.* **88**, 1475–1498 (1988). doi: 10.1021/cr00090a003
32. D. F. Parsons, B. W. Ninham, Ab initio molar volumes and Gaussian radii. *J. Phys. Chem. A* **113**, 1141–1150 (2009). doi: 10.1021/jp802984b; pmid: 19140766
33. D. V. Talapin, E. V. Shevchenko, C. B. Murray, A. V. Titov, P. Král, Dipole-dipole interactions in nanoparticle superlattices. *Nano Lett.* **7**, 1213–1219 (2007). doi: 10.1021/nl070058c; pmid: 17397231
34. E. V. Shevchenko, D. V. Talapin, N. A. Kotov, S. O'Brien, C. B. Murray, Structural diversity in binary nanoparticle superlattices. *Nature* **439**, 55–59 (2006). doi: 10.1038/nature04414; pmid: 16397494
35. Y. Qin, K. A. Fichthorn, Solvophobic solvation at large and intermediate length scales: Size, shape, and solvent effects. *Phys. Rev. E* **74**, 020401 (2006). doi: 10.1103/PhysRevE.74.020401; pmid: 17025385
36. S. Shanbhag, N. A. Kotov, On the origin of a permanent dipole moment in nanocrystals with a cubic crystal lattice: Effects of truncation, stabilizers, and medium for CdS tetrahedral homologues. *J. Phys. Chem. B* **110**, 12211–12217 (2006). doi: 10.1021/jp0611119; pmid: 16800539
37. Y. Qin, K. A. Fichthorn, Molecular dynamics simulation of the forces between colloidal nanoparticles in *n*-decane solvent. *J. Chem. Phys.* **127**, 144911 (2007). doi: 10.1063/1.2776259; pmid: 17935443
38. B. Bozorgui, D. Meng, S. K. Kumar, C. Chakravarty, A. Cacciuto, Fluctuation-driven anisotropic assembly in nanoscale systems. *Nano Lett.* **13**, 2732–2737 (2013). doi: 10.1021/nl401378r; pmid: 23713810
39. W. A. Ducker, T. J. Senden, R. M. Pashley, Direct measurement of colloidal forces using an atomic force microscope. *Nature* **353**, 239–241 (1991). doi: 10.1038/353239a0
40. S. L. Eichmann, S. G. Anekal, M. A. Bevan, Electrostatically confined nanoparticle interactions and dynamics. *Langmuir* **24**, 714–721 (2008). doi: 10.1021/la702571z; pmid: 18177058

41. L. Tong, V. D. Miljković, P. Johansson, M. Käll, Plasmon hybridization reveals the interaction between individual colloidal gold nanoparticles confined in an optical potential well. *Nano Lett.* **11**, 4505–4508 (2011). doi: 10.1021/nl1036116; pmid: 21142200
42. L. H. Allen, E. Matijević, Stability of colloidal silica. *J. Colloid Interface Sci.* **35**, 66–76 (1971). doi: 10.1016/0021-9797(71)90186-X
43. M. Kobayashi, M. Skarba, P. Galletto, D. Cakara, M. Borkovec, Effects of heat treatment on the aggregation and charging of Stöber-type silica. *J. Colloid Interface Sci.* **292**, 139–147 (2005). doi: 10.1016/j.jcis.2005.05.093; pmid: 16009370
44. J.-D. Hu *et al.*, Effect of dissolved organic matter on the stability of magnetite nanoparticles under different pH and ionic strength conditions. *Sci. Total Environ.* **408**, 3477–3489 (2010). doi: 10.1016/j.scitotenv.2010.03.033; pmid: 20421125
45. R. Huang, R. P. Carney, F. Stellacci, B. L. T. Lau, Colloidal stability of self-assembled monolayer-coated gold nanoparticles: The effects of surface compositional and structural heterogeneity. *Langmuir* **29**, 11560–11566 (2013). doi: 10.1021/la4020674; pmid: 23944688
46. F. J. Montes Ruiz-Cabello, G. Trefalt, P. Maroni, M. Borkovec, Accurate predictions of forces in the presence of multivalent ions by Poisson-Boltzmann theory. *Langmuir* **30**, 4551–4555 (2014). doi: 10.1021/la500612a; pmid: 24735066
47. V. Merk *et al.*, In situ non-DLVO stabilization of surfactant-free, plasmonic gold nanoparticles: Effect of Hofmeister's anions. *Langmuir* **30**, 4213–4222 (2014). doi: 10.1021/la404556a; pmid: 24720469
48. G. I. Guerrero-García, P. González-Mozuelos, M. Olvera de la Cruz, Large counterions boost the solubility and renormalized charge of suspended nanoparticles. *ACS Nano* **7**, 9714–9723 (2013). doi: 10.1021/nn404477b; pmid: 24180597
49. S. W. Bian, I. A. Mudunkotuwa, T. Rupasinghe, V. H. Grassian, Aggregation and dissolution of 4 nm ZnO nanoparticles in aqueous environments: Influence of pH, ionic strength, size, and adsorption of humic acid. *Langmuir* **27**, 6059–6068 (2011). doi: 10.1021/la200570n; pmid: 21500814
50. T. Laaksonen, P. Ahonen, C. Johans, K. Kontturi, Stability and electrostatics of mercaptoundecanoic acid-capped gold nanoparticles with varying counterion size. *ChemPhysChem* **7**, 2143–2149 (2006). doi: 10.1002/cphc.200600307; pmid: 16969881
51. M. Elimelech, C. R. O'Melia, Effect of electrolyte type on the electrophoretic mobility of polystyrene latex colloids. *Colloids Surf.* **44**, 165–178 (1990). doi: 10.1016/0166-6622(90)80194-9
52. C. Zukoski IV, D. Saville, The interpretation of electrokinetic measurements using a dynamic model of the stern layer. *J. Colloid Interface Sci.* **114**, 32–44 (1986). doi: 10.1016/0021-9797(86)90238-9
53. Y. Yu *et al.*, Nanocrystal superlattices that exhibit improved order on heating: An example of inverse melting? *Faraday Discuss.* **181**, 181–192 (2015). doi: 10.1039/C5FD00006H; pmid: 25930234
54. W. D. Luedtke, U. Landman, Structure, dynamics, and thermodynamics of passivated gold nanocrystallites and their assemblies. *J. Phys. Chem.* **100**, 13323–13329 (1996). doi: 10.1021/jp961721g
55. G. I. Guerrero-García, P. González-Mozuelos, M. Olvera de la Cruz, Potential of mean force between identical charged nanoparticles immersed in a size-asymmetric monovalent electrolyte. *J. Chem. Phys.* **135**, 164705 (2011). doi: 10.1063/1.3656763; pmid: 22047261
56. E. Heikkilä *et al.*, Atomistic simulations of functional Au 144 (SR) 60 gold nanoparticles in aqueous environment. *J. Phys. Chem. C* **116**, 9805–9815 (2012). doi: 10.1021/jp301094m
57. Y.-X. Yu, J. Wu, G.-H. Gao, Density-functional theory of spherical electric double layers and ζ potentials of colloidal particles in restricted-primitive-model electrolyte solutions. *J. Chem. Phys.* **120**, 7223–7233 (2004). doi: 10.1063/1.1676121; pmid: 15267630
58. S. Jenkins, S. R. Kirk, M. Persson, J. Carlen, Z. Abbas, Molecular dynamics simulation of nanocolloidal amorphous silica particles: Part II. *J. Chem. Phys.* **128**, 164711 (2008). doi: 10.1063/1.2906462; pmid: 18447483
59. N. A. Kotov, F. C. Meldrum, J. H. Fendler, Monoparticulate layers of titanium dioxide nanocrystallites with controllable interparticle distances. *J. Phys. Chem.* **98**, 8827–8830 (1994). doi: 10.1021/j100087a002
60. Y. Xia *et al.*, Self-assembly of self-limiting monodisperse supraparticles from polydisperse nanoparticles. *Nat. Nanotechnol.* **6**, 580–587 (2011). doi: 10.1038/nnano.2011.121; pmid: 21857686
61. S. Srivastava *et al.*, Light-controlled self-assembly of semiconductor nanoparticles into twisted ribbons. *Science* **327**, 1355–1359 (2010). doi: 10.1126/science.1177218; pmid: 20150443
62. J. Yeom *et al.*, Chiral templating of self-assembling nanostructures by circularly polarized light. *Nat. Mater.* **14**, 66–72 (2015). doi: 10.1038/nmat4125; pmid: 25401922
63. J. C. Ang *et al.*, Human serum albumin binding to silica nanoparticles – effect of protein fatty acid ligand. *Phys. Chem. Chem. Phys.* **16**, 10157–10168 (2014). doi: 10.1039/c4cp00293h; pmid: 24595605
64. L. Treuel *et al.*, Impact of protein modification on the protein corona on nanoparticles and nanoparticle-cell interactions. *ACS Nano* **8**, 503–513 (2014). doi: 10.1021/nn405019v; pmid: 24377255
65. P. K. Ghorai, S. C. Glotzer, Molecular dynamics simulation study of self-assembled monolayers of alkanethiol surfactants on spherical gold nanoparticles. *J. Phys. Chem. C* **111**, 15857–15862 (2007). doi: 10.1021/jp0746289
66. C. Singh *et al.*, Entropy-mediated patterning of surfactant-coated nanoparticles and surfaces. *Phys. Rev. Lett.* **99**, 226106–226109 (2007). doi: 10.1103/PhysRevLett.99.226106; pmid: 18233304
67. N. O. Fischer, C. M. McIntosh, J. M. Simard, V. M. Rotello, Inhibition of chymotrypsin through surface binding using nanoparticle-based receptors. *Proc. Natl. Acad. Sci. U.S.A.* **99**, 5018–5023 (2002). doi: 10.1073/pnas.082644099
68. D. Ishii *et al.*, Chaperonin-mediated stabilization and ATP-triggered release of semiconductor nanoparticles. *Nature* **423**, 628–632 (2003).
69. S.-H. Cha *et al.*, Shape-dependent biomimetic inhibition of enzyme by nanoparticles and their antibacterial activity. *ACS Nano* 10.1021/acsnano.5b03247 (2015). doi: 10.1021/acsnano.5b03247
70. P. del Pino *et al.*, Protein corona formation around nanoparticles – from the past to the future. *Mater. Horiz.* **1**, 301–313 (2014). doi: 10.1039/C3MH00106G
71. D. Horinek, R. R. Netz, Specific ion adsorption at hydrophobic solid surfaces. *Phys. Rev. Lett.* **99**, 226104 (2007). doi: 10.1103/PhysRevLett.99.226104; pmid: 18233302
72. N. Schwierz, D. Horinek, R. R. Netz, Anionic and cationic Hofmeister effects on hydrophobic and hydrophilic surfaces. *Langmuir* **29**, 2602–2614 (2013). doi: 10.1021/la303924e; pmid: 23339330
73. B. W. Ninham, P. Lo Nostro, *Molecular Forces and Self Assembly: In Colloid, Nano Sciences and Biology* (Cambridge Molecular Science series, Cambridge Univ. Press, Cambridge, 2010).
74. G. I. Guerrero García, M. Olvera de la Cruz, Polarization effects of dielectric nanoparticles in aqueous charge-asymmetric electrolytes. *J. Phys. Chem. B* **118**, 8854–8862 (2014). doi: 10.1021/jp5045173; pmid: 24953671
75. D. F. Parsons, M. Boström, T. J. Maceina, A. Salis, B. W. Ninham, Why direct or reversed Hofmeister series? Interplay of hydration, non-electrostatic potentials, and ion size. *Langmuir* **26**, 3323–3328 (2010). doi: 10.1021/la903061h; pmid: 20175572
76. A. P. dos Santos, Y. Levin, Ion specificity and the theory of stability of colloidal suspensions. *Phys. Rev. Lett.* **106**, 167801 (2011). doi: 10.1103/PhysRevLett.106.167801; pmid: 21599413
77. I. Kalcher, J. C. F. Schulz, J. Dzubiella, Ion-specific excluded-volume correlations and solvation forces. *Phys. Rev. Lett.* **104**, 097802 (2010). doi: 10.1103/PhysRevLett.104.097802; pmid: 20367012
78. R. R. Netz, Electrostatistics of counter-ions at and between planar charged walls: From Poisson-Boltzmann to the strong-coupling theory. *Eur. Phys. J. E* **5**, 557–574 (2001). doi: 10.1007/s101890170039
79. J. Forsman, A simple correlation-corrected Poisson–Boltzmann theory. *J. Phys. Chem. B* **108**, 9236–9245 (2004). doi: 10.1021/jp049571u
80. K. Besteman, M. A. Zevenbergen, S. G. Lemay, Charge inversion by multivalent ions: Dependence on dielectric constant and surface-charge density. *Phys. Rev. E* **72**, 061501–061510 (2005). doi: 10.1103/PhysRevE.72.061501; pmid: 16485949
81. G. I. Guerrero-García, E. González-Tovar, M. Olvera de la Cruz, Entropic effects in the electric double layer of model colloids with size-asymmetric monovalent ions. *J. Chem. Phys.* **135**, 054701 (2011). doi: 10.1063/1.3622046; pmid: 21823720
82. A. E. Larsen, D. G. Grier, Like-charge attractions in metastable colloidal crystallites. *Nature* **385**, 230–233 (1997). doi: 10.1038/385230a0
83. P. Sinha, I. Szilagyi, F. J. Montes Ruiz-Cabello, P. Maroni, M. Borkovec, Attractive forces between charged colloidal particles induced by multivalent ions revealed by confronting aggregation and direct force measurements. *J. Phys. Chem. Lett.* **4**, 648–652 (2013). doi: 10.1021/jz4000609; pmid: 26281881
84. D. Antypov, M. C. Barbosa, C. Holm, Incorporation of excluded-volume correlations into Poisson-Boltzmann theory. *Phys. Rev. E* **71**, 061106 (2005). doi: 10.1103/PhysRevE.71.061106
85. R. Kjellander, Intricate coupling between ion-ion and ion-surface correlations in double layers as illustrated by charge inversion-combined effects of strong Coulomb correlations and excluded volume. *J. Phys. Condens. Matter* **21**, 424101 (2009). doi: 10.1088/0953-8984/21/42/424101; pmid: 21715836
86. A. G. Moreira, R. R. Netz, Simulations of counterions at charged plates. *Eur. Phys. J. E* **8**, 33–58 (2002). pmid: 15010981
87. A. P. dos Santos, A. Diehl, Y. Levin, Electrostatic correlations in colloidal suspensions: Density profiles and effective charges beyond the Poisson-Boltzmann theory. *J. Chem. Phys.* **130**, 124110 (2009). doi: 10.1063/1.3098556; pmid: 19334811
88. F. J. Montes Ruiz-Cabello *et al.*, Long-ranged and soft interactions between charged colloidal particles induced by multivalent coions. *Soft Matter* **11**, 1562–1571 (2015). doi: 10.1039/C4SM02510E; pmid: 25590285
89. R. Messina, Electrostatics in soft matter. *J. Phys. Condens. Matter* **21**, 113102 (2009). doi: 10.1088/0953-8984/21/11/113102; pmid: 21693906
90. A. Sánchez-Iglesias *et al.*, Hydrophobic interactions modulate self-assembly of nanoparticles. *ACS Nano.* **6**, 11059–11065 (2012). pmid: 23186074
91. M. Zobel, R. B. Neder, S. A. J. Kimber, Universal solvent restructuring induced by colloidal nanoparticles. *Science* **347**, 292–294 (2015). doi: 10.1126/science.1261412; pmid: 25593188
92. G. Chopra, M. Levitt, Remarkable patterns of surface water ordering around polarized buckminsterfullerene. *Proc. Natl. Acad. Sci. U.S.A.* **108**, 14455–14460 (2011). doi: 10.1073/pnas.1110626108
93. S. Ebbinghaus *et al.*, An extended dynamical hydration shell around proteins. *Proc. Natl. Acad. Sci. U.S.A.* **104**, 20749–20752 (2007). doi: 10.1073/pnas.0709207104; pmid: 18093918
94. D. Chandler, Interfaces and the driving force of hydrophobic assembly. *Nature* **437**, 640–647 (2005). doi: 10.1038/nature04162; pmid: 16193038
95. J. G. Davis, K. P. Gierszal, P. Wang, D. Ben-Amotz, Water structural transformation at molecular hydrophobic interfaces. *Nature* **491**, 582–585 (2012). doi: 10.1038/nature11570; pmid: 23172216
96. J. G. Davis, B. M. Rankin, K. P. Gierszal, D. Ben-Amotz, On the cooperative formation of non-hydrogen-bonded water at molecular hydrophobic interfaces. *Nat. Chem.* **5**, 796–802 (2013). doi: 10.1038/nchem.1716; pmid: 23965683
97. B. M. Rankin, D. Ben-Amotz, Expulsion of ions from hydrophobic hydration shells. *J. Am. Chem. Soc.* **135**, 8818–8821 (2013). doi: 10.1021/ja4036303; pmid: 23734747
98. A. J. Patel *et al.*, Sitting at the edge: How biomolecules use hydrophobicity to tune their interactions and function. *J. Phys. Chem. B* **116**, 2498–2503 (2012). doi: 10.1021/jp2107523; pmid: 22235927
99. H.-Y. Kim, J. O. Sofo, D. Velegol, M. W. Cole, G. Mukhopadhyay, Static polarizabilities of dielectric nanoclusters. *Phys. Rev. A* **72**, 053201 (2005). doi: 10.1103/PhysRevA.72.053201
100. J. H. Bahng *et al.*, Anomalous dispersions of 'hedgehog' particles. *Nature* **517**, 596–599 (2015). doi: 10.1038/nature14092; pmid: 25631447
101. H.-Y. Kim, P. R. C. Kent, van der Waals forces: Accurate calculation and assessment of approximate methods in dielectric nanocolloids up to 16 nm. *J. Chem. Phys.* **131**, 144705 (2009). doi: 10.1063/1.3244645; pmid: 19831462
102. H. Y. Kim, J. O. Sofo, D. Velegol, M. W. Cole, A. A. Lucas, Van der Waals dispersion forces between dielectric nanoclusters. *Langmuir* **23**, 1735–1740 (2007). doi: 10.1021/la061802w; pmid: 17279651

103. H.-Y. Kim, J. O. Sofo, D. Velegol, M. W. Cole, A. A. Lucas, van der Waals forces between nanoclusters: Importance of many-body effects. *J. Chem. Phys.* **124**, 074504 (2006). doi: 10.1063/1.2170091; pmid: 16497054
104. W. Sun, Q. Zeng, A. Yu, Calculation of noncontact forces between silica nanospheres. *Langmuir* **29**, 2175–2184 (2013). doi: 10.1021/la305156s; pmid: 23339620
105. A. White, J. F. Dobson, Enhanced dispersion interaction between quasi-one-dimensional conducting collinear structures. *Phys. Rev. B* **77**, 075436 (2008). doi: 10.1103/PhysRevB.77.075436
106. L. E. Brus, A simple model for the ionization potential, electron affinity, and aqueous redox potentials of small semiconductor crystallites. *J. Chem. Phys.* **79**, 5566 (1983). doi: 10.1063/1.445676
107. W. Szczerba, H. Riesemeier, A. F. Thünemann, Bond length contraction in gold nanoparticles. *Anal. Bioanal. Chem.* **398**, 1967–1972 (2010). doi: 10.1007/s00216-010-4200-z; pmid: 20848088
108. A. M. Jackson, J. W. Myerson, F. Stellacci, Spontaneous assembly of subnanometre-ordered domains in the ligand shell of monolayer-protected nanoparticles. *Nat. Mater.* **3**, 330–336 (2004). doi: 10.1038/nmat1116; pmid: 15098025
109. P. Guo, R. Sknepnek, M. Olvera de la Cruz, Electrostatic-driven ridge formation on nanoparticles coated with charged end-group ligands. *J. Phys. Chem. C* **115**, 6484–6490 (2011). doi: 10.1021/jp201598k
110. M. R. Jones, R. J. Macfarlane, A. E. Prigodich, P. C. Patel, C. A. Mirkin, Nanoparticle shape anisotropy dictates the collective behavior of surface-bound ligands. *J. Am. Chem. Soc.* **133**, 18865–18869 (2011). doi: 10.1021/ja206777k; pmid: 22043984
111. A. P. Kaushik, P. Clancy, Explicit all-atom modeling of realistically sized ligand-capped nanocrystals. *J. Chem. Phys.* **136**, 114702 (2012). doi: 10.1063/1.3689973; pmid: 22443785
112. M. A. Boles, D. V. Talapin, Many-body effects in nanocrystal superlattices: Departure from sphere packing explains stability of binary phases. *J. Am. Chem. Soc.* **137**, 4494–4502 (2015). doi: 10.1021/jacs.5b00839; pmid: 25773648
113. B. S. Jabes, H. O. S. Yadav, S. K. Kumar, C. Chakravarty, Fluctuation-driven anisotropy in effective pair interactions between nanoparticles: Thiolated gold nanoparticles in ethane. *J. Chem. Phys.* **141**, 154904 (2014). doi: 10.1063/1.4897541; pmid: 25338910
114. A. Widmer-Cooper, P. Geissler, Orientational ordering of passivating ligands on CdS nanorods in solution generates strong rod-rod interactions. *Nano Lett.* **14**, 57–65 (2014). doi: 10.1021/nl403067p; pmid: 24295449
115. M. Dzugutov, Glass formation in a simple monatomic liquid with icosahedral inherent local order. *Phys. Rev. A* **46**, R2984–R2987 (1992). doi: 10.1103/PhysRevA.46.R2984; pmid: 9908539
116. U. Landman, W. D. Luedtke, Small is different: Energetic, structural, thermal, and mechanical properties of passivated nanocluster assemblies. *Faraday Discuss.* **125**, 1–22 (2004). doi: 10.1039/b312640b; pmid: 14750661
117. C. R. Iacovella, A. S. Keys, S. C. Glotzer, Self-assembly of soft-matter quasicrystals and their approximants. *Proc. Natl. Acad. Sci. U.S.A.* **108**, 20935–20940 (2011). doi: 10.1073/pnas.1019763108; pmid: 22160672
118. D. V. Talapin *et al.*, Quasicrystalline order in self-assembled binary nanoparticle superlattices. *Nature* **461**, 964–967 (2009). doi: 10.1038/nature08439; pmid: 19829378
119. H.-Y. Lee *et al.*, Self-assembly of nanoparticle amphiphiles with adaptive surface chemistry. *ACS Nano* **8**, 9979–9987 (2014). doi: 10.1021/nn504734v; pmid: 25229312
120. Z. Nie *et al.*, Self-assembly of metal-polymer analogues of amphiphilic triblock copolymers. *Nat. Mater.* **6**, 609–614 (2007). doi: 10.1038/nmat1954; pmid: 17618291
121. J. He, Y. Liu, T. Babu, Z. Wei, Z. Nie, Self-assembly of inorganic nanoparticle vesicles and tubules driven by tethered linear block copolymers. *J. Am. Chem. Soc.* **134**, 11342–11345 (2012). doi: 10.1021/ja3032295; pmid: 22746265
122. G. U. Kulkarni, P. J. Thomas, C. N. R. Rao, Mesoscale organization of metal nanocrystals. *Pure Appl. Chem.* **74**, 1581–1591 (2002). doi: 10.1351/pac200274091581
123. T. Geyer, P. Born, T. Kraus, Switching between crystallization and amorphous agglomeration of alkyl thiol-coated gold nanoparticles. *Phys. Rev. Lett.* **109**, 128302 (2012). doi: 10.1103/PhysRevLett.109.128302; pmid: 23005995
124. J. J. Gray, B. Chiang, R. T. Bonnecaze, Colloidal particles: Origin of anomalous multibody interactions. *Nature* **402**, 750 (1999).
125. A. Haji-Akbari *et al.*, Disordered, quasicrystalline and crystalline phases of densely packed tetrahedra. *Nature* **462**, 773–777 (2009). doi: 10.1038/nature08641; pmid: 20010683
126. J. Huang, F. Kim, A. R. Tao, S. Connor, P. Yang, Spontaneous formation of nanoparticle stripe patterns through dewetting. *Nat. Mater.* **4**, 896–900 (2005). doi: 10.1038/nmat1517; pmid: 16284621
127. K. D. Hermanson, S. O. Lumsdon, J. P. Williams, E. W. Kaler, O. D. Velev, Dielectrophoretic assembly of electrically functional microwires from nanoparticle suspensions. *Science* **294**, 1082–1086 (2001). doi: 10.1126/science.1063821;pmid: 11691987
128. G. Singh *et al.*, Self-assembly of magnetite nanocubes into helical superstructures. *Science* **345**, 1149–1153 (2014). doi: 10.1126/science.1254132; pmid: 25061133
129. C. Pfeiffer *et al.*, Interaction of colloidal nanoparticles with their local environment: The (ionic) nanoenvironment around nanoparticles is different from bulk and determines the physico-chemical properties of the nanoparticles. *J. R. Soc. Interface* **11**, 20130931 (2014).pmid: 24759541
130. M. van der Linden *et al.*, Microscopic origin of the Hofmeister effect in gelation kinetics of colloidal silica. *J. Phys. Chem. Lett.* **6**, 2881–2887 (2015). doi: 10.1021/acs.jpclett.5b01300; pmid: 26267174
131. C. Wagner *et al.*, Non-additivity of molecule-surface van der Waals potentials from force measurements. *Nat. Commun.* **5**, 5568 (2014). doi: 10.1038/ncomms6568; pmid: 25424490
132. Q. Chen *et al.*, Interaction potentials of anisotropic nanocrystals from the trajectory sampling of particle motion using in situ liquid phase transmission electron microscopy. *ACS Cent. Sci.* **1**, 33–39 (2015). doi: 10.1021/acscentsci.5b00001
133. H. E. Sauceda *et al.*, Vibrational properties of metal nanoparticles: Atomistic simulation and comparison with time-resolved investigation. *J. Phys. Chem. C* **116**, 25147–25156 (2012). doi: 10.1021/jp309499t
134. J. J. Torres-Vega, L. R. Medrano, C. V. Landauro, J. Rojas-Tapia, Determination of the threshold of nanoparticle behavior: Structural and electronic properties study of nano-sized copper. *Physica B* **436**, 74–79 (2014). doi: 10.1016/j.physb.2013.11.036
135. P. K. Naicker, P. T. Cummings, H. Zhang, J. F. Banfield, Characterization of titanium dioxide nanoparticles using molecular dynamics simulations. *J. Phys. Chem. B* **109**, 15243–15249 (2005). doi: 10.1021/jp050963q; pmid: 16852930
136. V. A. Parsegian, *Van der Waals Forces* (Cambridge Univ. Press, Cambridge, 2006).
137. I. E. Dzyaloshinskii, E. M. Lifshitz, L. P. Pitaevskii, The general theory of van der Waals forces. *Adv. Phys.* **10**, 165–209 (1961). doi: 10.1080/00018736100101281
138. E. K. Hobbie, T. Ihle, J. M. Harris, M. R. Semler, Empirical evaluation of attractive van der Waals potentials for type-purified single-walled carbon nanotubes. *Phys. Rev. B* **85**, 245439 (2012). doi: 10.1103/PhysRevB.85.245439
139. R. Rajter, R. H. French, Van der Waals-London dispersion interaction framework for experimentally realistic carbon nanotube systems. *Int. J. Mater. Res.* **101**, 27–42 (2010). doi: 10.3139/146.110250
140. B. Faure, G. Salazar-Alvarez, L. Bergström, Hamaker constants of iron oxide nanoparticles. *Langmuir* **27**, 8659–8664 (2011). doi: 10.1021/la201387d; pmid: 21644514
141. A. O. Pinchuk, Size-dependent hamaker constant for silver nanoparticles. *J. Phys. Chem. C* **116**, 20099–20102 (2012). doi: 10.1021/jp3061784
142. Y. Andersson, D. C. Langreth, B. I. Lundqvist, van der Waals interactions in density-functional theory. *Phys. Rev. Lett.* **76**, 102–105 (1996). doi: 10.1103/PhysRevLett.76.102; pmid: 10060444
143. J. Tao, J. P. Perdew, A. Ruzsinszky, Accurate van der Waals coefficients from density functional theory. *Proc. Natl. Acad. Sci. U.S.A.* **109**, 18–21 (2012). doi: 10.1073/pnas.1118245108; pmid: 22205765
144. V. V. Gobre, A. Tkatchenko, Scaling laws for van der Waals interactions in nanostructured materials. *Nat. Commun.* **4**, 2341 (2013). doi: 10.1038/ncomms3341; pmid: 23955481
145. M. Dijkstra, Computer simulations of charge and steric stabilised colloidal suspensions. *Curr. Opin. Colloid Interface Sci.* **6**, 372–382 (2001). doi: 10.1016/S1359-0294(01)00106-6

ACKNOWLEDGMENTS

This work was supported by the Multidisciplinary University Research Initiative project from the U.S. Department of Defense (grant W911NF-10-1-0518, "Reconfigurable Matter from Programmable Colloids") and the Emerging Frontiers in Research and Innovation–BioSensing and BioActuation grant 0938019 project of the NSF. Partial support was also provided by the Center for Photonic and Multiscale Nanomaterials (C-PHOM) funded by the NSF Materials Research Science and Engineering Center program Division of Materials Research (DMR) grant 1120923; NSF Chemical, Bioengineering, Environmental, and Transport Systems (CBET) grants 1036672, 1403777, 1463474, and 1538180; and DMR grant 1411014. C.A.S.B. and N.A.K. acknowledge a Presidential Fellowship from the University of Michigan.

10.1126/science.1242477

Nonadditivity of nanoparticle interactions

Carlos A. Silvera Batista, Ronald G. Larson and Nicholas A. Kotov

Science **350** (6257), 1242477.
DOI: 10.1126/science.1242477

Solutions for nanoparticle solutions

Nanoparticle interactions in solution affect their binding to biomolecules, their electronic properties, and their packing into larger crystals. However, the theories that describe larger colloidal particles fail for nanoparticles, because the interactions do not add together linearly. Nanoparticles also have complex shapes and are closer in size to the solvent molecules. Silvera Batista *et al.* review approaches that can treat the nonadditive nature of nanoparticle interactions, resulting in a more complete understanding of nanoparticles in solution.

Science, this issue p. 10.1126/science.1242477